Chapter 2
Förster-Type Nonradiative Energy Transfer Rates for Nanostructures with Various Dimensionalities

In this chapter, we derive the energy transfer rate for the cases of X → NP (nanoparticle), X → NW (nanowire), and X → QW (quantum well), where X is an NP, an NW, or a QW, and obtain simply expression for the long distance approximation. This chapter is reprinted (adapted) with permission from Ref. [1]. Copyright 2013 American Chemical Society.

We need to recall the results in Chap. 5 from Understanding and Modeling Förster-type Resonance Energy Transfer (FRET) Vol. 1, where the Fermi's Golden Rule is simplified into

$$\gamma_{trans} = \frac{2}{\hbar} \operatorname{Im}\left[\int dV \left(\frac{\varepsilon_A(\omega)}{4\pi}\right) \mathbf{E}_{in}(\mathbf{r}) \cdot \mathbf{E}_{in}^{*}(\mathbf{r})\right] \tag{2.1}$$

And

$$\mathbf{E}(\mathbf{r}) = -\nabla\Phi(\mathbf{r}) \tag{2.2}$$

with

$$\Phi_{\alpha}(\mathbf{r}) = \left(\frac{ed_{exc}}{\varepsilon_{eff_D}}\right) \frac{(\mathbf{r} - \mathbf{r}_0) \cdot \hat{\boldsymbol{\alpha}}}{|\mathbf{r} - \mathbf{r}_0|^3} \tag{2.3}$$

In addition to the previous results, we also recall the results obtained in the previous chapter (Chap. 1) regarding to the effective dielectric constant summarized in Table 2.1.

P.L. Hernández Martínez et al., *Understanding and Modeling Förster-type Resonance Energy Transfer (FRET)*, Nanoscience and Nanotechnology,
DOI 10.1007/978-981-10-1873-2_2

Table 2.1 Effective dielectric constant expressions for the cases of an NP, an NW, and a QW in the long distance approximation [Reprinted (adapted) with permission from Ref. [1] (Copyright 2013 American Chemical Society)]

α-direction	NP	NW	QW
x	$\varepsilon_{eff_D} = \frac{\varepsilon_{NP_D} + 2\varepsilon_0}{3}$	$\varepsilon_{eff_D} = \frac{\varepsilon_{NW} + \varepsilon_0}{2}$	$\varepsilon_{eff_D} = \varepsilon_0$
y	$\varepsilon_{eff_D} = \frac{\varepsilon_{NP_D} + 2\varepsilon_0}{3}$	$\varepsilon_{eff_D} = \varepsilon_0$	$\varepsilon_{eff_D} = \varepsilon_0$
z	$\varepsilon_{eff_D} = \frac{\varepsilon_{NP_D} + 2\varepsilon_0}{3}$	$\varepsilon_{eff_D} = \frac{\varepsilon_{NW} + \varepsilon_0}{2}$	$\varepsilon_{eff_D} = \varepsilon_0$

2.1 Cases of Förster-Type Energy Transfer to an Nanoparticle: NP → NP, NW → NP, and QW → NP

Here, we report analytical equations for FRET rate when the donor is an NP, an NW, or a QW and the acceptor is always an NP (Fig. 2.1). Furthermore, for the long distance approximation, we obtain simplified expressions for the transfer rate for all three cases (NP → NP, NW → NP, and QW → NP).

The exciton transfer rate (2.1), when the acceptor is an NP, is given by

$$\gamma_{\alpha,\,trans} = \frac{2}{\hbar}\,\mathrm{Im}\left[\int_{NP_A} dV\left(\frac{\varepsilon_{NP_A}(\omega)}{4\pi}\right)\mathbf{E}_{\alpha,\,in}(\mathbf{r})\cdot\mathbf{E}^{*}_{\alpha,\,in}(\mathbf{r})\right] \tag{2.4}$$

where ε_{NP_A} is the dielectric function of the acceptor and $\mathbf{E}_{\alpha,\,in}(\mathbf{r})$ is the induced electric field of an α-exciton ($\alpha = x,\, y,\, z$) in the donor. Assuming that the donor size is smaller than the separation distance between D and A and using the spherical symmetry of the acceptor, the total electric potential for the acceptor can be written as

$$\Phi^{out}_{\alpha}(r,\,\theta,\,\phi) = \Phi_{\alpha}(r,\,\theta,\,\phi) + \sum_{l,m}\frac{B^{\alpha}_{l,m}}{r^{l+1}}Y_{l,\,m}(\theta,\,\phi) \tag{2.5}$$

$$\Phi^{in}_{\alpha}(r,\,\theta,\,\phi) = \sum_{l,m}A^{\alpha}_{l,m}r^{l}Y_{l,\,m}(\theta,\,\phi) \tag{2.6}$$

where $\Phi_{\alpha}(r,\,\theta,\,\phi)$ is the electric potential of the exciton in the donor; $Y_{l,\,m}(\theta,\,\phi)$ are the spherical harmonics; and $A^{\alpha}_{l,m}$ and $B^{\alpha}_{l,m}$ are the coefficients determined by the boundary conditions. For the spherical case, the boundary conditions at the acceptor's surface ($r = R_{NP_A}$) are

$$\Phi^{in}_{\alpha}(r = R_{NP_A},\,\theta,\,\phi) = \Phi^{out}_{\alpha}(r = R_{NP_A},\,\theta,\,\phi) \tag{2.7}$$

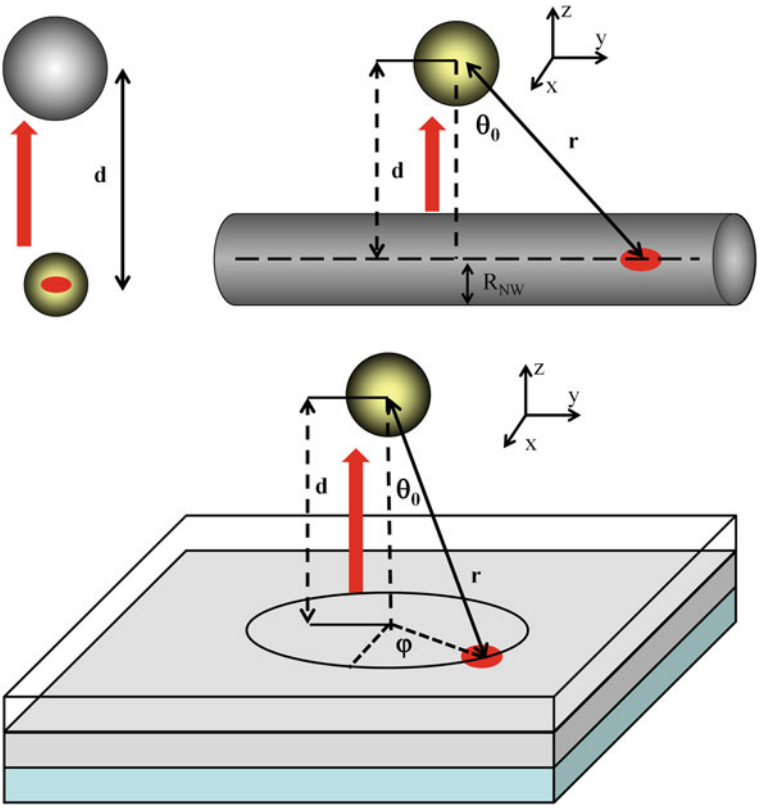

Fig. 2.1 Schematic for the energy transfer of NP → NP, NW → NP, and QW → NP. *Red arrows* show the energy transfer direction. *Red circles* represent an exciton in the α-direction. d is the separation distance. θ_0 is the azimuthal angle between d and r. φ is the radial angle [Reprinted (adapted) with permission from Ref. [1] (Copyright 2013 American Chemical Society)]

$$\varepsilon_{in}\left[\frac{\partial\Phi_{\alpha}^{in}(r,\,\theta,\,\phi)}{\partial r}\right]_{r=R_{NP_A}}=\varepsilon_{out}\left[\frac{\partial\Phi_{\alpha}^{out}(r,\,\theta,\,\phi)}{\partial r}\right]_{r=R_{NP_A}} \tag{2.8}$$

where $\varepsilon_{in(out)}$ is the dielectric function inside (outside) the acceptor. Applying the boundary conditions (2.7) and (2.8) in (2.5) and (2.6), we obtain:

$$A_{l,m}^{\alpha}=\frac{B_{l,m}^{\alpha}}{R_{NP_A}^{2l+1}}+\frac{f_{l,m}^{\alpha}}{R_{NP_A}^{l}} \tag{2.9}$$

$$B_{l,m}^{\alpha}=\frac{R_{NP_A}^{l+2}\left(\varepsilon_{out}g_{l,m}^{\alpha}-l\varepsilon_{in}\frac{f_{l,m}^{\alpha}}{R_{NP_A}}\right)}{l\varepsilon_{in}+(l+1)\,\varepsilon_{out}} \tag{2.10}$$

with $f_{l.m}^{\alpha}$ and $g_{l.m}^{\alpha}$, which are given by

$$f_{l,m}^{\alpha} = \int_0^{2\pi} \int_0^{\pi} \left[\Phi_{\alpha}(r,\ \theta,\ \phi)\right]_{r=R_{NP_A}} Y_{l,m}^{*}(\theta,\ \phi) \sin(\theta)\, d\theta d\phi \tag{2.11}$$

$$g_{l,m}^{\alpha} = \int_0^{2\pi} \int_0^{\pi} \left[\frac{\partial \Phi_{\alpha}(r,\ \theta,\ \phi)}{\partial r}\right]_{r=R_{NP_A}} Y_{l,m}^{*}(\theta,\ \phi) \sin(\theta)\, d\theta d\phi \tag{2.12}$$

and $\varepsilon_{out} = \varepsilon_0$ is the dielectric constant of the medium, and $\varepsilon_{in} = \varepsilon_{NP_A}$ is the dielectric function of the acceptor. Combining (2.6) and (2.2) into (2.4), we obtain the energy transfer rate as

$$\gamma_{\alpha,\,trans} = \frac{2}{\hbar} \mathrm{Im}\left[\varepsilon_{NP_A}(\omega)\left(\frac{1}{4\pi}\right) \sum_{l,m} \left|A_{l,m}^{\alpha}\right|^2 \cdot l \cdot R_{NP_A}^{2l+1}\right] \tag{2.13}$$

where $A_{l,m}^{\alpha}$ is given by (2.9). This is a general expression, which is valid under the assumption mentioned above. From (2.13), we observe that the distance dependency for the transfer rate is given by the coefficient $A_{l,m}^{\alpha}$. Now we derive an asymptotic behavior (long distance limit) for the transfer rate in the dipole approximation for: (1) NP → NP; (2) NW → NP; and (3) QW → NP. In all cases, we assume that the donor size is small compared to the separation distance d. Under this condition, the NP-to-NP transfer rate $(\gamma_{\alpha,\,trans})$ is

$$\gamma_{\alpha,\,trans} = \frac{2}{\hbar} b_{\alpha} \left(\frac{e d_{exc}}{\varepsilon_{eff_D}}\right)^2 \frac{R_{NP_A}^3}{d^6} \left|\frac{3\varepsilon_0}{\varepsilon_{NP_A}(\omega_{exc}) + 2\varepsilon_0}\right|^2 \mathrm{Im}\left[\varepsilon_{NP_A}(\omega_{exc})\right] \tag{2.14}$$

where $b_{\alpha} = \frac{1}{3}, \frac{1}{3}, \frac{4}{3}$ for $\alpha = x, y, z$, respectively; d is the center-to-center distance between the donor and acceptor; and ε_{eff_D} the effective dielectric constant for the exciton in the donor, which is equal to $\varepsilon_{eff_D} = \frac{\varepsilon_{NP_D} + 2\varepsilon_0}{3}$ (Table 2.1) for the NP → NP case.

The transfer rate $(\gamma_{\alpha,\,trans})$ for the NW → NP is

$$\gamma_{\alpha,\,trans} = \frac{2}{\hbar} b_{\alpha} \left(\frac{e d_{exc}}{\varepsilon_{eff_D}}\right)^2 \frac{R_{NP_A}^3}{d^6} \cos^6(\theta_0) \left|\frac{3\varepsilon_0}{\varepsilon_{NP_A}(\omega_{exc}) + 2\varepsilon_0}\right|^2 \mathrm{Im}\left[\varepsilon_{NP_A}(\omega_{exc})\right] \tag{2.15}$$

where $b_{\alpha} = \frac{1}{3}, \frac{1}{3}, \frac{4}{3}$ for $\alpha = x, y, z$, respectively; θ_0 is the angle between d and $\mathbf{r}$; ε_{eff_D} the effective dielectric constant for the exciton in the donor, which is equal to

$\varepsilon_{eff_D} = \varepsilon_0$ for $\alpha = y$ (parallel to the cylindrical axis) and $\varepsilon_{eff_D} = \frac{\varepsilon_{NW}+\varepsilon_0}{2}$, $\alpha = x, z$ (perpendicular to the cylindrical axis) (Table 2.1).

Similarly, for the QW → NP, $\gamma_{\alpha,trans}$ is

$$\gamma_{\alpha,trans} = \frac{2}{\hbar} b_\alpha \left(\frac{e d_{exc}}{\varepsilon_{eff_D}}\right)^2 \frac{R^3_{NP_A}}{d^6} \cos^6(\theta_0) \left|\frac{3\varepsilon_0}{\varepsilon_{NP_A}(\omega_{exc}) + 2\varepsilon_0}\right|^2 \mathrm{Im}\left[\varepsilon_{NP_A}(\omega_{exc})\right] \quad (2.16)$$

where $b_\alpha = \frac{1}{3}, \frac{1}{3}, \frac{4}{3}$ for $\alpha = x, y, z$, respectively; θ_0 is the angle between d and $\mathbf{r}$; and ε_{eff_D} the effective dielectric constant for the exciton in the donor, which is equal to $\varepsilon_{eff_D} = \varepsilon_0$ for $\alpha = x, y, z$ (Table 2.1).

The FRET rate for the NP → NP case follows the well-known asymptotic behavior $\gamma \propto d^{-6}$ [2]. Furthermore, the FRET rates are proportional to the imaginary part of the acceptor dielectric constant. Thus, an acceptor with strong absorption (large $\mathrm{Im}\,|\varepsilon_{NP_A}(\omega)|$) will have higher transfer rates. Moreover, in the cases of NW-to-NP and QW-to-NP, the transfer rate strongly depends on the distance and θ_0. In particular for the angle dependency, the main contribution comes from small θ_0 and decreases very fast as θ_0 increases. It is important to note that the transfer rate in these cases (NW-to-NP and QW-to-NP) follows the same distance dependency as the NP-to-NP transfer rate, which is $\gamma \propto d^{-6}$ [2]. These results suggest that the NRET rates are dictated by the acceptor's dimensionality, but not the donor's. It is worth mentioning that the FRET rate for the NW → NP and QW → NP cases have not been reported in early works. However, these missing cases for the FRET rates were reported in Ref. [1].

To illustrate the FRET rate, we present the average FRET rate in the long distance approximation as a function of the distance between CdTe D–A pair in Fig. 2.2. The acceptor dielectric function is taken from Ref. [3]. We assume that the acceptor exciton emission is at $\lambda = 582$ nm. In Fig. 2.2a, we consider the donor to be an NP, an NW, or a QW and the acceptor to be an NP. We set $\theta_0 = 0$ for the NP-to-NW and NP-to-QW cases. In this particular model, the larger average transfer rate is for the QW-to-NP case, and the smaller average transfer rate is for the NP-to-NP case. Figure 2.2c shows the energy transfer rate for the QW-to-NP case. Figure 2.2d depicts the contour profile plot for the QW-to-NP transfer rate. The top panel in Fig. 2.2d illustrates the energy transfer rate as a function of the distance at a fixed angle. Blue curve represents the case at $\theta_0 = 0$, and wine curve, at $\theta_0 = \pi/6$. The right panel in Fig. 2.2d shows the transfer rate as a function of the angle at a fixed distance. Red curve represents the case at $d = 3.3$ nm, and the green curve, at $d = 4.0$ nm. From Fig. 2.2c, d, the strong distance dependency of the transfer rate (2.15 and 2.16) is observed. Therefore, the main contribution for the energy transfer from a QW(NW) to an NP comes at short distances and small angles.

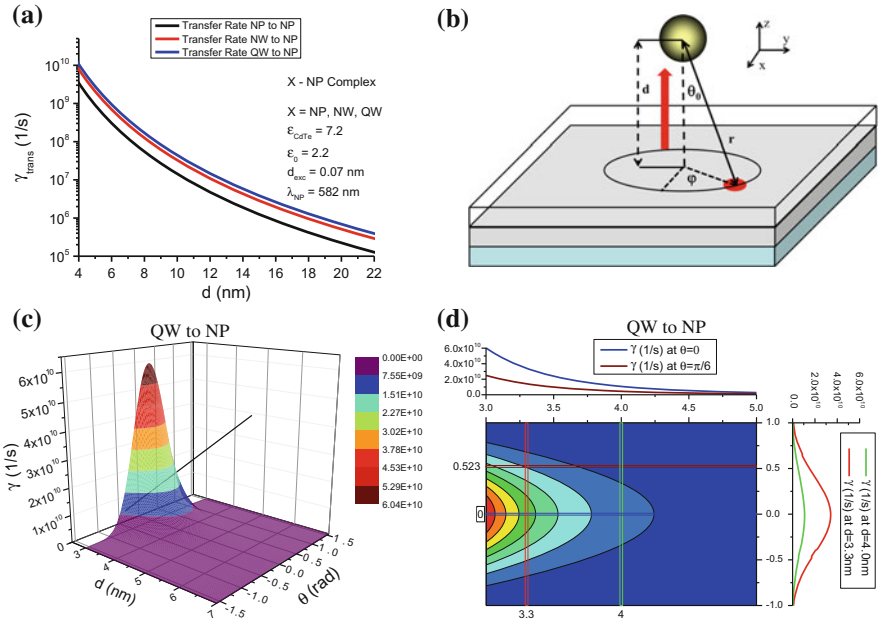

Fig. 2.2 **a** Average FRET rate for CdTe D–A pair. This shows the distance dependency of FRET rate for the NP → NP, NW → NP, and QW → NP cases. $\theta_0 = 0$ for the NW → NP and QW → NP pairs. **b** Schematic for the energy transfer of QW → NP case. **c** Average FRET rate for the CdTe D–A QW → NP pair as a function of the distance and angle. **d** Contour profile map for the average FRET rate for the CdTe D–A QW → NP pair, with the *top panel* at a fixed angle and *right panel* at a fixed distance [Reprinted (adapted) with permission from Ref. [1] (Copyright 2013 American Chemical Society)]

2.2 Cases of Förster-Type Energy Transfer to an Nanowire: NP → NW, NW → NW, and QW → NW

Here, we obtain analytical equations for the FRET rate when the donor is an NP, an NW, or a QW while the acceptor is always an NW (Fig. 2.3). We also obtained the simplified expressions for FRET rate in the long distance approximation for all these cases.

The transfer rate (2.1), when the acceptor is an NW, is written as

$$\gamma_{\alpha,trans} = \frac{2}{\hbar}\,\mathrm{Im}\left[\int_{NW_A} dV\left(\frac{\varepsilon_{NW_A}(\omega)}{4\pi}\right)\mathbf{E}_{\alpha,in}(\mathbf{r})\cdot\mathbf{E}^{*}_{\alpha,in}(\mathbf{r})\right] \tag{2.17}$$

Here $\mathbf{E}_{\alpha,in}(\mathbf{r})$ is the induced electric field of an α-exciton ($\alpha = x, y, z$) in the donor and ε_{NW} is the dielectric function of the acceptor (NW). We assume that the

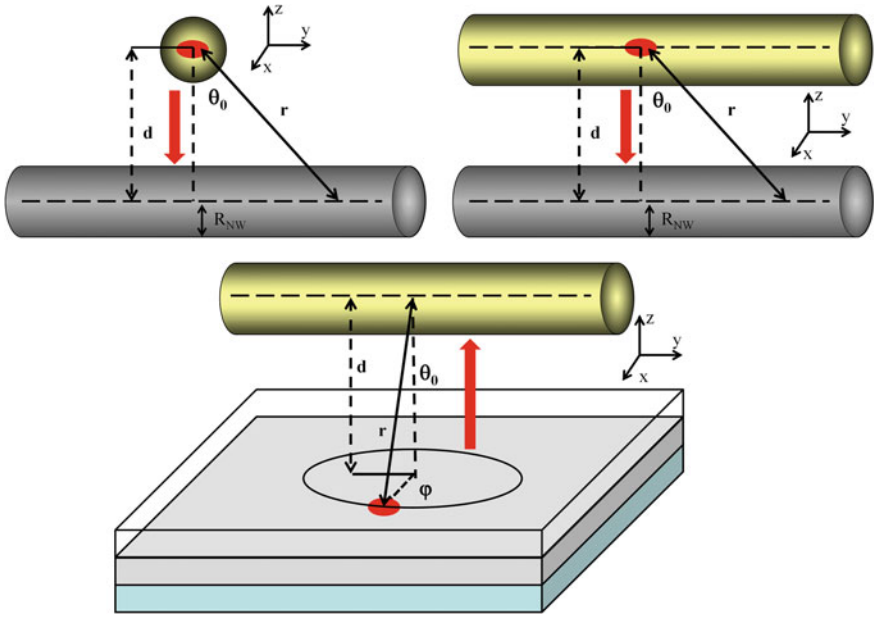

Fig. 2.3 Schematic for the energy transfer of NP → NW, NW → NW, and QW → NW. *Red arrows* show the energy transfer direction. *Red circles* represent an exciton in the α-direction. d is the separation distance. θ_0 is the azimuthal angle between d and r. φ is the radial angle [Reprinted (adapted) with permission from Ref. [1] (Copyright 2013 American Chemical Society)]

donor size is small compared to the D–A separation distance d. Taking advantage of the cylindrical symmetry of the acceptor, the total electric potential for the acceptor can be written as

$$\Phi_{\alpha}^{out}(\rho,\,\phi,\,z) = \Phi_{\alpha}(\rho,\,\phi,\,z) + \sum_{m} \int_{-\infty}^{\infty} dk \mathrm{e}^{-\mathrm{i}kz} B_{m}^{\alpha}(k) K_{m}(|k\,|\,\rho) \mathrm{e}^{\mathrm{i}m\phi} \tag{2.18}$$

$$\Phi_{\alpha}^{in}(\rho,\,\phi,\,z) = \sum_{m} \int_{-\infty}^{\infty} dk \mathrm{e}^{-\mathrm{i}kz} A_{m}^{\alpha}(k) I_{m}(|k\,|\,\rho) \mathrm{e}^{\mathrm{i}m\phi} \tag{2.19}$$

where $\Phi_{\alpha}(\rho,\,\phi,\,z)$ is the electric potential of the exciton in the donor; $I_m(|k\,|\,\rho)$ and $K_m(|k\,|\,\rho)$ are the modified Bessel functions; and $A_m^{\alpha}(k)$ and $B_m^{\alpha}(k)$ are the coefficients determined by the boundary conditions. For the cylindrical case, the boundary conditions at the acceptor's surface $(\rho = R_{NW_A})$ are

$$\Phi_{\alpha}^{in}(\rho = R_{NW_A},\,\phi,\,z) = \Phi_{\alpha}^{out}(\rho = R_{NW_A},\,\phi,\,z) \tag{2.20}$$

$$\varepsilon_{in}\left[\frac{\partial\Phi_{\alpha}^{in}(\rho,\,\phi,\,z)}{\partial\rho}\right]_{\rho=R_{NW_A}}=\varepsilon_{out}\left[\frac{\partial\Phi_{\alpha}^{out}(\rho,\,\phi,\,z)}{\partial\rho}\right]_{\rho=R_{NW_A}} \tag{2.21}$$

where $\varepsilon_{in(out)}$ is the dielectric function inside (outside) the acceptor. Applying the boundary conditions (2.20) and (2.21) in (2.18) and (2.19), we arrive at

$$A_m^{\alpha}(k)=\frac{K_m(|k\,|\,R_{NW_A})}{I_m(|k\,|\,R_{NW_A})}B_m^{\alpha}(k)+\frac{f_m^{\alpha}(|k|)}{I_m(|k\,|\,R_{NW_A})} \tag{2.22}$$

$$B_m^{\alpha}(k)=\frac{\frac{2}{|k|}\varepsilon_{out}g_m^{\alpha}(|k|)-\varepsilon_{in}\frac{I_m'(|k\,|\,R_{NW_A})}{I_m(|k\,|\,R_{NW_A})}f_m^{\alpha}(|k|)}{\varepsilon_{in}\left(\frac{I_m'(|k\,|\,R_{NW_A})}{I_m(|k\,|\,R_{NW_A})}\right)K_m(|k\,|\,R_{NW_A})+\varepsilon_{out}K_m'(|k\,|\,R_{NW_A})} \tag{2.23}$$

with $I_m(|k\,|\,R_{NW_A})$, $K_m(|k\,|\,R_{NW_A})$, f_m^{α}, and g_m^{α} given by

$$I_m(|k\,|\,R_{NW_A})=I_{m+1}(|k\,|\,R_{NW_A})+I_{m-1}(|k\,|\,R_{NW_A}) \tag{2.24}$$

$$K_m(|k\,|\,R_{NW_A})=K_{m+1}(|k\,|\,R_{NW_A})+K_{m-1}(|k\,|\,R_{NW_A}) \tag{2.25}$$

$$f_m^{\alpha}=\frac{1}{(2\pi)^2}\int_0^{2\pi}\int_{-\infty}^{\infty}[\Phi_{\alpha}(\rho,\,\phi,\,z)]_{\rho=R_{NW_A}}\mathrm{e}^{\mathrm{i}kz}\mathrm{e}^{-\mathrm{i}m\phi}\,dzd\phi \tag{2.26}$$

$$g_m^{\alpha}=\frac{1}{(2\pi)^2}\int_0^{2\pi}\int_{-\infty}^{\infty}\left[\frac{\partial\Phi_{\alpha}(\rho,\,\phi,\,z)}{\partial\rho}\right]_{\rho=R_{NW_A}}\mathrm{e}^{\mathrm{i}kz}\mathrm{e}^{-\mathrm{i}m\phi}dzd\phi \tag{2.27}$$

and $\varepsilon_{out}=\varepsilon_0$ is the dielectric constant of the medium, and $\varepsilon_{in}=\varepsilon_{NW_A}$ is the dielectric function of the NW. Combining (2.19) and (2.2) into (2.17), we obtain that the energy transfer rate of

$$\gamma_{\alpha,\,trans}=\frac{2}{\hbar}\,\mathrm{Im}\left[\frac{\varepsilon_{NW_A}(\omega_{exc})}{4\pi}\right](2\pi)^2\sum_m\int_{-\infty}^{\infty}dk|A_m^{\alpha}(|k|)|^2$$
$$\times\left(\frac{|k|^2}{4}\int_0^{R_{NW_A}}|I_m(|k\,|\,\rho)|^2\rho d\rho+m^2\int_0^{R_{NW_A}}|I_m(|k\,|\,\rho)|^2\frac{1}{\rho}d\rho+|k|^2\int_0^{R_{NW_A}}|I_m(|k\,|\,\rho)|^2\rho d\rho\right) \tag{2.28}$$

where $A_m^{\alpha}(k)$ is given by (2.22). This is a general expression, which is valid under the mentioned assumptions. Note that the distance dependency of FRET rate is given by the coefficient $A_m^{\alpha}(k)$. For the long distance approximation, we derive the

transfer rate equations for the NP-to-NW, NW-to-NW and QW-to-NW cases. Thus, the transfer rate is

$$\gamma_{\alpha,\,trans} = \frac{2}{\hbar}\left(\frac{ed_{exc}}{\varepsilon_{eff_D}}\right)^2\left(\frac{3\pi}{32}\right)\frac{R_{NW_A}^2}{d^5}\left(a_\alpha + b_\alpha\left|\frac{2\varepsilon_0}{\varepsilon_{NW_A}(\omega_{exc})+\varepsilon_0}\right|^2\right)\mathrm{Im}\left[\varepsilon_{NW_A}(\omega_{exc})\right] \tag{2.29}$$

where $a_\alpha = 0, \frac{9}{16}, \frac{15}{16}$; $b_\alpha = 1, \frac{15}{16}, \frac{41}{16}$ for $\alpha = x, y, z$, respectively; d is the center-to-center distance between the donor and the acceptor; and ε_{eff_D} is the effective dielectric constant for the exciton in the donor, which is equal to $\varepsilon_{eff_D} = \frac{\varepsilon_{NP_D}+2\varepsilon_0}{3}$ for NP $\rightarrow$ NW. In the NW $\rightarrow$ NW case, the effective dielectric constant is $\varepsilon_{eff_D} = \varepsilon_0$ for $\alpha = y$ (parallel to the cylindrical axis) and $\varepsilon_{eff_D} = \frac{\varepsilon_{NW_D}+\varepsilon_0}{2}$ for $\alpha = x, z$ (perpendicular to the cylindrical axis) (Table 2.1). Likewise, the QW-to-NW transfer rate $(\gamma_{\alpha,\,trans})$ is given by

$$\gamma_{\alpha,\,trans} = \frac{2}{\hbar}\left(\frac{ed_{exc}}{\varepsilon_{eff_D}}\right)^2\left(\frac{3\pi}{32}\right)\frac{R_{NW_A}^2}{d^5}\cos^5(\theta_0)\left(a_\alpha + b_\alpha\left|\frac{2\varepsilon_0}{\varepsilon_{NW_A}(\omega_{exc})+\varepsilon_0}\right|^2\right)\mathrm{Im}\left[\varepsilon_{NW_A}(\omega_{exc})\right] \tag{2.30}$$

where θ_0 is the angle between d and $\mathbf{r}$ and ε_{eff_D} is the effective dielectric constant for the exciton in the donor, which is equal to $\varepsilon_{eff_D} = \varepsilon_0$ for $\alpha = x, y, z$ (Table 2.1).

As expected, the asymptotic behavior for the NRET rate of the QW $\rightarrow$ NW case follows $\gamma \propto d^{-5}$ [1]. This result is similar to the NP-to-NW and NW-to-NW cases, as reported in Refs. [4, 5], respectively. Similar to the previous section, the FRET rates strongly depend on the distance and θ_0, and a similar analysis can be made. Figure 2.4a depicts the average FRET rate for a CdTe D–A pair as a function of the distance, when the donor is an NP, an NW, or a QW while the acceptor is an NW in all cases. We set $\theta_0 = 0$ for the QW-to-NW case. We assume that the acceptor exciton emission is at $\lambda = 610$ nm and the acceptor dielectric function is taken from Ref. [3]. Note that the higher transfer rate is for the QW-to-NW, and the lower rate is for the NP-to-NW. Figure 2.4c, d depict the average FRET rate for a CdTe D–A pair as a function of the distance and θ_0, when the donor is a QW and the acceptor is an NW. Figure 2.4d shows the contour profile map for the QW-to-NW transfer rate. The top panel in Fig. 2.4d illustrates the energy transfer rate as a function of the distance at a fixed angle. Blue curve represents the case at $\theta_0 = 0$, and wine curve, at $\theta_0 = \pi/6$. The right panel in Fig. 2.4d shows the transfer rate as a function of the angle at a fixed distance. Red curve represents the behavior at $d = 3.3$ nm, and the green curve, at $d = 4.0$ nm. From Fig. 2.4a, c, d, show the strong distance dependency of the transfer rate (2.29, 2.30). Similar to the previous section, the main contribution for the energy transfer from a QW to an NW comes at short distances and small angles.

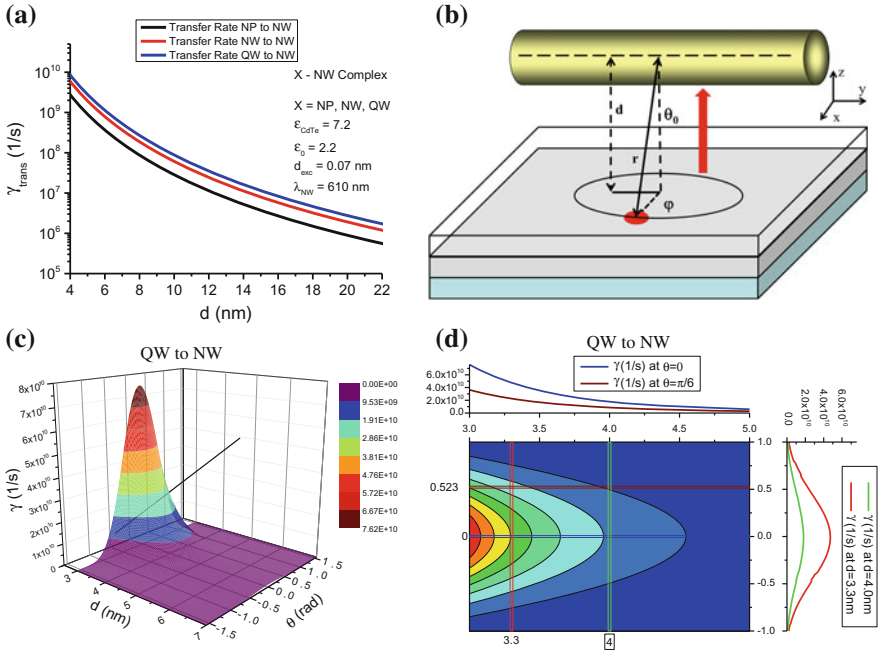

Fig. 2.4 **a** Average FRET rate for CdTe D–A pair. This plot illustrates the FRET distance dependency for NP → NW, NW → NW, and QW → NW cases. $\theta_0 = 0$ for QW to NW pairs. **b** Schematic for the energy transfer of QW → NW case. **c** Average FRET rate for the CdTe D–A QW → NW pair as a function of the distance and angle. **d** Contour profile map for the average FRET rate of QW → NW, with the *top panel* at a fixed angle, and the *right panel* at a fixed distance [Reprinted (adapted) with permission from Ref. [1] (Copyright 2013 American Chemical Society)]

2.3 Cases of Förster-Type Energy Transfer to a Quantum Well: NP → QW, NW → QW, and QW → QW

In this section, we obtain analytical equations for the FRET rate when the donor is an NP, an NW, or a QW while the acceptor is always a QW (Fig. 2.5). Moreover, the simplified expression for the FRET rate in the long distance approximation is obtained for all these cases.

The transfer rate (2.1), when the acceptor is a QW, is written as

$$\gamma_{\alpha,trans} = \frac{2}{\hbar}\,\mathrm{Im}\left[\int_{QW_A} dV\left(\frac{\varepsilon_{QW_A}(\omega)}{4\pi}\right)\mathbf{E}_{\alpha,in}(\mathbf{r})\cdot\mathbf{E}^{*}_{\alpha,in}(\mathbf{r})\right] \tag{2.31}$$

where $\mathbf{E}_{\alpha,in}(\mathbf{r})$ represents the electric field of an α-exciton ($\alpha = x, y, z$) in the donor and ε_{QW_A} is the dielectric function of the acceptor (QW). Now we assume that the

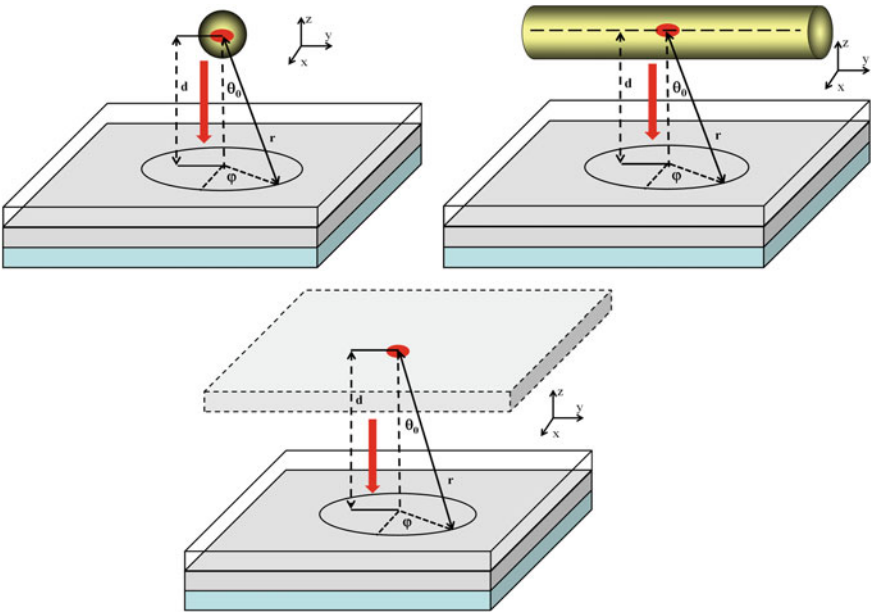

Fig. 2.5 Schematic for the energy transfer of NP → QW, NW → QW, and QW → QW. *Red arrows* show the energy transfer direction. *Red circles* represent an exciton in the α-direction. d is the separation distance. θ_0 is the azimuthal angle between d and r. φ is the radial angle [Reprinted (adapted) with permission from Ref. [1] (Copyright 2013 American Chemical Society)]

donor size is small compared to the D–A separation distance d. Furthermore, we consider a symmetric structure, consisting of a semiconductor QW of thickness L_w between two barriers of dielectric function ε_{QW_A}. One barrier has a film thickness L_l, while the other barrier is considered to be very thick (where we assume that this barrier is semi-infinite). The donor nanostructure is placed in front of the barrier with thickness L_l and we solve the problem for the case where the QW is very thin ($L_w \ll L_l$). Under these assumptions, the electric potential inside the barrier is

$$\Phi_{in}(\mathbf{r}) = \left(\frac{2\varepsilon_0}{\varepsilon_{QW_A} + \varepsilon_0}\right) \Phi_\alpha(\mathbf{r}) \tag{2.32}$$

where ε_0 is the dielectric constant of the matrix (surrounding the medium around the donor); ε_{QW_A} is the dielectric function of the barrier; and Φ_α is the electric potential of an α-exciton in the donor nanostructure. Combining (2.32) and (2.2) into (2.31), we obtain

$$\gamma_{\alpha,\,trans} = \frac{2}{\hbar}\left|\frac{2\varepsilon_0}{\varepsilon_{QW_A} + \varepsilon_0}\right|^2 \mathrm{Im}\left[\int dV \left(\frac{\varepsilon_{QW_A}(\omega)}{4\pi}\right) \mathbf{E}_\alpha(\mathbf{r}) \cdot \mathbf{E}_\alpha^*(\mathbf{r})\right] \tag{2.33}$$

where $E_\alpha(\mathbf{r})$ is the electric field created by an α-exciton in the donor. By using the assumption that the QW is very thin ($L_w \ll L_l$), the energy transfer rate becomes

$$\gamma_{\alpha,trans} = \frac{2}{\hbar}\left|\frac{2\varepsilon_0}{\varepsilon_{QW_A}+\varepsilon_0}\right|^2 \mathrm{Im}\left[\int_{QW_A} dS\left(\frac{\varepsilon_{QW_A}(\omega)}{4\pi}\right)\mathbf{E}_\alpha(\mathbf{r})\cdot\mathbf{E}^*_\alpha(\mathbf{r})\right] \tag{2.34}$$

where the integration is over the entire surface of the QW. In particular, we obtain the analytical expression for the long distance approximation for NP → QW, NW → QW, and QW → QW. In all cases, we assume $d_b \gg L_W$ where d_b is the distance from the center of the donor to the dielectric barrier. Under these conditions, $\gamma_{\alpha,trans}$ becomes

$$\gamma_{\alpha,trans} = \frac{2}{\hbar}b_\alpha\left(\frac{ed_{exc}}{\varepsilon_{eff_D}}\right)^2\frac{1}{d^4}\left|\frac{2\varepsilon_0}{\varepsilon_{QW_A}+\varepsilon_0}\right|^2 \mathrm{Im}\left[\varepsilon_{QW_A}(\omega_{exc})\right] \tag{2.35}$$

where $b_\alpha = \frac{3}{16}, \frac{3}{16}, \frac{3}{8}$ for $\alpha = x, y, z$, respectively; $d = d_b + L_l$ is the distance between the donor and the acceptor; and ε_{eff_D} is the effective dielectric constant for the exciton in the donor, which is equal to $\varepsilon_{eff_D} = \frac{\varepsilon_{NP_D}+2\varepsilon_0}{3}$ for NP → QW. In the NW → QW case, the effective dielectric constant is $\varepsilon_{eff_D} = \varepsilon_0$ for $\alpha = y$ (parallel to the cylindrical axis) and $\varepsilon_{eff_D} = \frac{\varepsilon_{NW}+\varepsilon_0}{2}$ for $\alpha = x, z$ (perpendicular to the cylindrical axis). For QW→QW, $\varepsilon_{eff_D} = \varepsilon_0$ for $\alpha = x, y, z$ (Table 2.1). Note that the FRET rate for the NP → QW and QW → QW cases follow the well-known asymptotic behavior $\gamma \propto d^{-4}$ [6] and $\gamma \propto d^{-4}$ [7], respectively. Akin to the previous cases for the FRET rate, we have included the FRET rate for the NW → QW case, which was studied in Ref. [1].

Figure 2.6 shows the average FRET rate for a CdTe D–A pair as a function of the distance, when the donor is an NP, an NW, or a QW with the acceptor being a

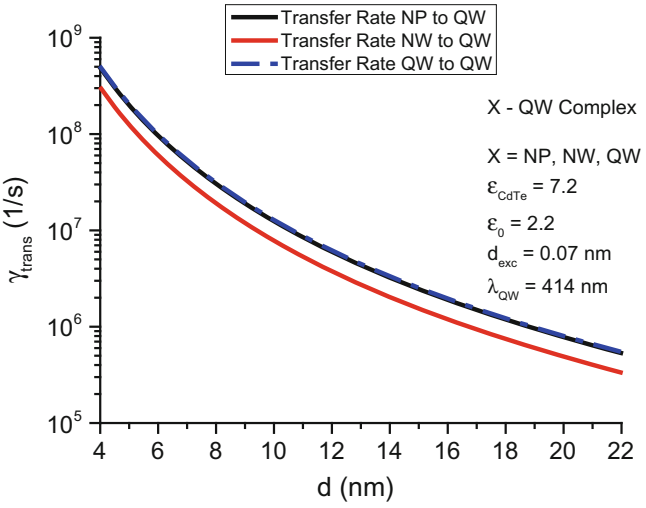

Fig. 2.6 Average FRET rate for a CdTe D–A pair. This plot shows the distance dependency of the FRET rate for the NP → QW, NW → QW, and QW → QW cases [Reprinted (adapted) with permission from Ref. [1] (Copyright 2013 American Chemical Society)]

QW in all cases. In this plot, we made similar assumptions as the previous section. Here, the faster transfer rate is for the QW → QW pair which slightly faster than the NP → QW pair; On the other hand, the lower transfer rate is for the NW → QW pair.

2.4 Example: Energy Transfer Between Nanoparticles and Nanowires

As an example we calculate Förster energy transfer from an optically excited NP to NW as shown in Fig. 2.7 [4]. The center-to-center distance between NP and NW is denoted as d, and the distance between the NP center and the NW surface is given by Δ. A NW, NP, and matrix are described with local dielectric constants denoted as $\varepsilon_{NW}, \varepsilon_{NP}$, and ε_0, respectively. The local dielectric constant approach provides us with a reliable description if the transferred exciton energy when the bandgap of a donor nanocrystal is not very close to the bandgap of a NW (acceptor). From (2.28), the transfer rate takes the form Ref. [4]

$$\gamma_\alpha = \frac{2}{\hbar}\,\mathrm{Im}\left[\frac{\varepsilon_{NW}}{2\pi}\right]\cdot(2\pi)^2\sum_m \int_{-\infty}^{\infty} dk\,|A^*(m,k)|^2 \times\left\{\frac{k^2}{4}\int_0^{R_{NW}} \rho d\rho\,|I_{m+1}(k\rho)+I_{m-1}(k\rho)|^2 + m^2\int_0^{R_{NW}}\frac{1}{\rho}d\rho\,|I_m(k\rho)|^2 + k^2\int_0^{R_{NW}}\rho d\rho\,|I_m(k\rho)|^2\right\} \tag{2.36}$$

For the case where $d \gg R_{NW}$, we expand (2.36) in terms of the parameter R_{NW}/d and obtain a convenient relation:

$$\gamma_\alpha(\omega_{exc}) = \frac{2}{\hbar}\frac{R_{NW}^2}{d^5}\left(\frac{e d_{exc}}{\varepsilon_{eff}}\right)^2\frac{3\pi}{32}\left(a_\alpha + \left|\frac{\varepsilon_0}{\varepsilon_{NW}+\varepsilon_0}\right|^2 b_\alpha\right)\mathrm{Im}\,\varepsilon_{NW} \tag{2.37}$$

where the coefficient a_α is 15/16, 0, and 9/16 for $\alpha = x, y$ and z, respectively; the corresponding values for the coefficient b_α are: 41/4, 4, and 15/4. Notice that the

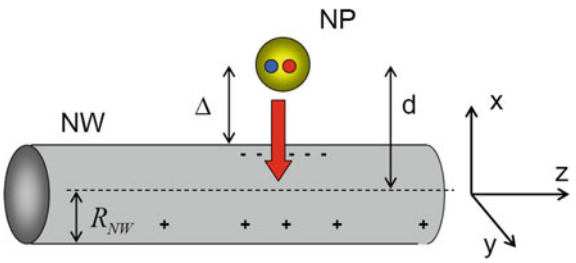

Fig. 2.7 Schematics of the coupled NP-NW system [Reprinted (abstract/excerpt/figure) with permission from Ref. [4] (Copyright 2008 by the American Physical Society)]

distance dependence of Förster transfer for the dipole-to-nanowire case is $\gamma_\alpha \propto 1/d^5$ as compared to the case of traditional dipole-dipole transfer $\gamma_{dipole-dipole} \propto 1/d^6$ [8, 9]. Slower spatial decay of the energy transfer rate comes from the one-dimensional character of a NW. Equation (2.36) is rather complicated, therefore (2.37) can be very convenient to estimate transfer rates in structures where $(R_{NW}/d) < 1$.

To illustrate the validity of (2.37), we numerically calculate the transfer rate for the cases of (1) CdTe NP–CdTe NW and (2) CdTe NP–Carbon Nanotube (CNT). In Fig. 2.8 shows the results for these complexes. The CdTe NPs and CdTe NWs was assembled and optically characterized in Ref. [10]. Experimental values for the FRET rates for NPs to NWs case were extracted from the photoluminescence spectra recorded during the assembly process. The experiment in Ref. [10] was performed with orange- and green-emitting CdTe NPs: $\lambda_{exc,orange\,NP} = 582$ nm ($R_{orange\,NP} = 2$ nm) and $\lambda_{exc,green\,NP} = 526$ nm ($R_{green\,NP} = 1.6$ nm). The NW radius $R_{NW} = 3.3$ nm and its emission is at $\lambda_{exc,NW} = 689$ nm. The NP-NW complex was assembled using the biotin-streptavidin biolinker with a length of 5 nm. The resultant NP-NW distances were estimated as: $d_{orange\,NP} = 10.3$ nm and $d_{green\,NP} = 9.9$ nm, with an estimated dipole moment of $d_{exc} \sim 0.08nm$. From the experiment, it was determined that $\gamma_{trans,\,orange} = 1/16\,\mathrm{ns}^{-1}$ and $\gamma_{trans,\,green} = 1/12\,\mathrm{ns}^{-1}$ whereas the corresponding theoretical estimated values are: $\gamma^{theory}_{trans,\,orange} \approx 1/13.1\,\mathrm{ns}^{-1}$ and $\gamma^{theory}_{trans,\,green} \approx 1/9\,\mathrm{ns}^{-1}$. From here, we can say that the calculations provide us with reliable estimates for the FRET rates for NP→NW system (Figs. 2.7

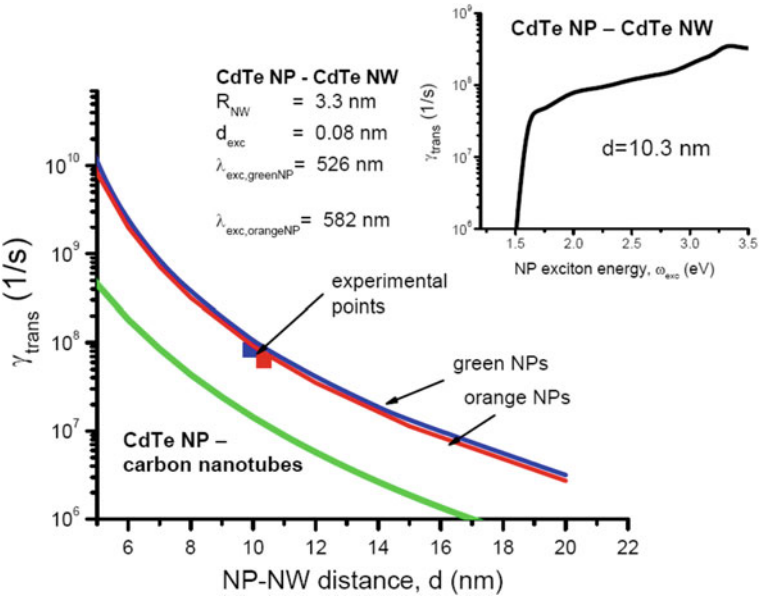

Fig. 2.8 Rates of NP-NW transfer of excitons as a function of the CdTe NP-NW separation and available experimental data from Ref. [10]. *Green line* shows the calculated rate for carbon nanotubes. *Inset* FRET rate for the NP-NW complex as a function of the exciton energy of a NP [Reprinted (abstract/excerpt/figure) with permission from Ref. [4] (Copyright 2008 by the American Physical Society)]

and 2.8). Figure 2.8 shows the dependence $\gamma_{trans}(\omega_{exc}, d = 10.3\ \text{nm})$ as an inset. The function $\gamma_{trans}(\omega_{exc})$ reflects the frequency dispersion of the CdTe dielectric function, $\varepsilon_{NW} = \varepsilon_{CdTe}(\omega)$. The CdTe NPs and CNTs we can neglect the second term in (2.37) because of the strong depolarization effect for the electric field perpendicular to the CNT axis [11]. Therefore, equation takes the form:

$$\gamma_{\alpha}(\omega_{exc}) = a_{\alpha}\frac{2}{\hbar}\frac{R_{CNT}^2}{d^5}\left(\frac{ed_{exc}}{\varepsilon_{eff}}\right)^2\frac{3\pi}{32}\,\text{Im}\,\varepsilon_{CNT} \tag{2.38}$$

where ε_{CNT} is the "z" component of the dielectric constant averaged over a CNT volume and the averaged transfer rate is given by $\gamma_{trans}(\omega_{exc}) = (3/2)\gamma_0$. Note that NP → CNT transfer is slower compared to that for the NP–NW system due to the smaller effective cross-section of CNT compared to the CdTe NW. This section is reprinted (abstract/excerpt/figure) with permission from Ref. [4]. Copyright 2008 by the American Physical Society.

2.5 Summary

To summarize the FRET rates, Table 2.2 lists the transfer rates for the long distance asymptotic behavior in the dipole approximation. Table 2.2 illustrates the distance dependency for the FRET: (1) when the acceptor is an NP, FRET is inversely

Table 2.2 FRET rate summary for the long distance asymptotic limit

α-direction	Donor			Coefficients		Acceptor distance dependency
	NP	NW	QW			X → NP
x	$\varepsilon_{eff_D} = \frac{\varepsilon_{NP_D}+2\varepsilon_0}{3}$	$\varepsilon_{eff_D} = \frac{\varepsilon_{NW}+\varepsilon_0}{2}$	$\varepsilon_{eff_D} = \varepsilon_0$	$b_x = \frac{1}{3}$		$\gamma_{NP} \propto \frac{1}{d^6}$
y	$\varepsilon_{eff_D} = \frac{\varepsilon_{NP_D}+2\varepsilon_0}{3}$	$\varepsilon_{eff_D} = \varepsilon_0$	$\varepsilon_{eff_D} = \varepsilon_0$	$b_y = \frac{1}{3}$		
z	$\varepsilon_{eff_D} = \frac{\varepsilon_{NP_D}+2\varepsilon_0}{3}$	$\varepsilon_{eff_D} = \frac{\varepsilon_{NW}+\varepsilon_0}{2}$	$\varepsilon_{eff_D} = \varepsilon_0$	$b_z = \frac{4}{3}$		
	NP	NW	QW			X → NW
x	$\varepsilon_{eff_D} = \frac{\varepsilon_{NP_D}+2\varepsilon_0}{3}$	$\varepsilon_{eff_D} = \frac{\varepsilon_{NW}+\varepsilon_0}{2}$	$\varepsilon_{eff_D} = \varepsilon_0$	$a_x = 0$	$b_x = 1$	$\gamma_{NW} \propto \frac{1}{d^5}$
y	$\varepsilon_{eff_D} = \frac{\varepsilon_{NP_D}+2\varepsilon_0}{3}$	$\varepsilon_{eff_D} = \varepsilon_0$	$\varepsilon_{eff_D} = \varepsilon_0$	$a_y = \frac{9}{16}$	$b_y = \frac{15}{16}$	
z	$\varepsilon_{eff_D} = \frac{\varepsilon_{NP_D}+2\varepsilon_0}{3}$	$\varepsilon_{eff_D} = \frac{\varepsilon_{NW}+\varepsilon_0}{2}$	$\varepsilon_{eff_D} = \varepsilon_0$	$a_z = \frac{15}{16}$	$b_z = \frac{41}{16}$	
	NP	NW	QW			X → QW
x	$\varepsilon_{eff_D} = \frac{\varepsilon_{NP_D}+2\varepsilon_0}{3}$	$\varepsilon_{eff_D} = \frac{\varepsilon_{NW}+\varepsilon_0}{2}$	$\varepsilon_{eff_D} = \varepsilon_0$	$b_x = \frac{3}{16}$		$\gamma_{QW} \propto \frac{1}{d^4}$
y	$\varepsilon_{eff_D} = \frac{\varepsilon_{NP_D}+2\varepsilon_0}{3}$	$\varepsilon_{eff_D} = \varepsilon_0$	$\varepsilon_{eff_D} = \varepsilon_0$	$b_y = \frac{3}{16}$		
z	$\varepsilon_{eff_D} = \frac{\varepsilon_{NP_D}+2\varepsilon_0}{3}$	$\varepsilon_{eff_D} = \frac{\varepsilon_{NW}+\varepsilon_0}{2}$	$\varepsilon_{eff_D} = \varepsilon_0$	$b_z = \frac{3}{8}$		

This list shows the distance dependence of the FRET rate as a function of the acceptor's geometry. Also, this includes the effective dielectric constant effect, which is a function of the donor's geometry. X = NP, NW or QW [Reprinted (adapted) with permission from Ref. [1]. (Copyright 2013 American Chemical Society)]

proportional to d^{-6} (2.14, 2.15, and 2.16); (2) when the acceptor is a NW, FRET is proportional to d^{-5} ((2.29) and (2.30)); and (3) when the acceptor is a QW, FRET is proportional to d^{-4} (2.35). This indicates that the donor dimensionality does not affect the functional distance dependency on the distance. To complete our analysis, Fig. 2.9a show the distance dependencies, given in Table 2.2. The energy transfer rates are presented as a function of d/d_0, where d_0 is the characteristic distance, which satisfies the asymptotic condition required for each case $\left(d \gg R_{NP,(NW)},\, d \gg L_{QW}\right)$. Figure 2.9b presents the energy transfer efficiency for the FRET as a function of d/d_0. In all cases, the FRET's distance dependency is given by the acceptor geometry and it is independent of the donor's geometry. Note

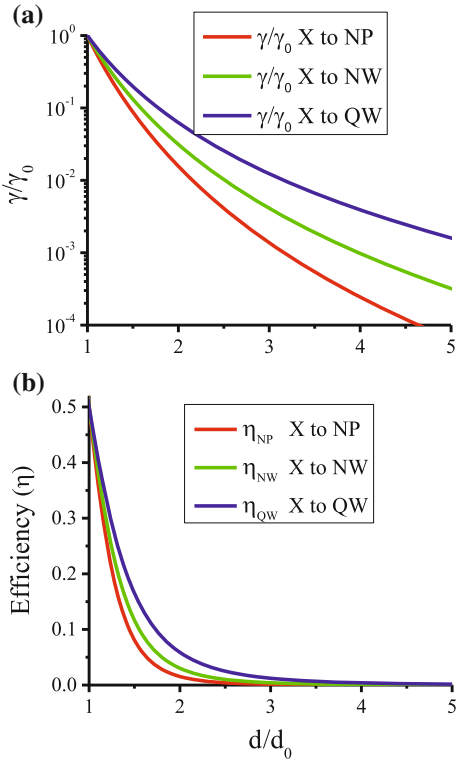

Fig. 2.9 **a** FRET rate distance dependency in the long distance asymptotic limit. Energy transfer rates are plotted as a function of d/d_0, where d_0 is the characteristic distance, which satisfies the asymptotic condition required for each case $\left(d \gg R_{NP,(NW)},\, d \gg L_{QW}\right)$. **b** Energy transfer efficiency for the FRET in the long distance asymptotic limit. Energy transfer efficiencies are plotted as a function of d/d_0. *Red line* shows the energy transfer efficiency for the D–A pair, when the acceptor is an NP. *Green line* depicts the energy transfer efficiency for the D–A pair when the acceptor is an NW. *Blue line* gives the energy transfer efficiency for the D–A pair when the acceptor is a QW. X = NP, NW, or QW [Reprinted (adapted) with permission from Ref. [1] (Copyright 2013 American Chemical Society)]

that the effective dielectric constant, however, depends only on the donor's geometry. Therefore, we can conclude that the FRET's distance dependency is dictated by the geometry of the acceptor nanostructure whereas the donor's contribution to the FRET appears through the effective dielectric constant. The dependencies given in Table 2.2 and Fig. 2.9 are important to understand FRET, and they are valid for the cases when the donor–donor and acceptor–acceptor separation distance is larger compared to the donor–acceptor separation distance. However, this condition is difficult to archieve experimentally and most of the experiments (in solid phase) are set using assembly of nanostructures. Therefore, it is crucial to understand FRET for the cases when the nanocrystals (NP and NW) are assembled into arrays (e.g., chains and films). This aspect is discussed in the following chapter.

References

1. P.L. Hernández-Martínez, A.O. Govorov, H.V. Demir, Generalized theory of Förster-type nonradiative energy transfer in nanostructures with mixed dimensionality. J. Phys. Chem. C **117**, 10203–10212 (2013)
2. A.O. Govorov, G.W. Bryant, W. Zhang, T. Skeini, J. Lee, N.A. Kotov, J.M. Slocik, R.R. Naik, Exciton-Plasmon interaction and hybrid excitons in semiconductor-metal nanoparticle assemblies. Nano Lett. **6**, 984–994 (2006)
3. E.D. Palik, *Handbook of Optical Constant of Solid* (Academic Press, New York, 1985)
4. P.L. Hernández-Martínez, A.O. Govorov, Exciton energy transfer between nanoparticles and nanowires. Phys. Rev. B **78**, 035314/1–035314/7 (2008)
5. S.K. Lyo, Exciton energy transfer between asymmetric quantum wires: effect of transfer to an array of wires. Phys. Rev. B **73**, 205322/1–205322/11 (2006)
6. S. Lu, A. Madhukar, Nonradiative resonant excitation transfer from nanocrystal quantum dots to adjacent quantum channels. Nano Lett. **7**, 3443–3451 (2007)
7. S.K. Lyo, Energy transfer from an electron-hole plasma layer to a quantum well in semiconductor structures. Phys. Rev. B **81**, 115303/1–115303/7 (2010)
8. D.L. Dexter, R.S. Knox, *Excitons* (Interscience Publishers, 1965)
9. T. Förster, in *Modern Quantum Chemistry*, ed. by O. Sinanoglu (Academic, New York, 1965)
10. J. Lee, A.O. Govorov, N.A. Kotov, Bioconjugated superstructures of CdTe nanowires and nanoparticles: multistep Cascade Förster resonance energy transfer and energy channeling. Nano Lett. **5**, 2063–2069 (2005)
11. C.D. Spataru, S. Ismail-beigi, X. Benedict, S.G. Louie, Appl. Phys. A **78**, 1129 (2004)

Springer

http://www.springer.com/978-981-10-1871-8

Understanding and Modeling Förster-type Resonance Energy Transfer (FRET)
FRET from Single Donor to Single Acceptor and Assemblies of Acceptors, Vol. 2
Hernández Martínez, P.L.; Govorov, A.; Demir, H.V.
2017, VI, 42 p. 15 illus. in color., Softcover
ISBN: 978-981-10-1871-8